

# Enhanced Thermal Conductance of ORU Radiant Fin Thermal Interface using Carbon Brush Materials

Christopher L. Seaman, Brett M. Ellman, and Timothy R. Knowles

*Energy Science Laboratories Inc., 6888 Nancy Ridge Dr., San Diego, CA 92121-2232, (619) 552-2039*

**Abstract.** ESLI has developed a highly compliant carbon brush thermal interface with good conductive heat transfer during a Phase 2 SBIR contract with NASA JSC. This lightweight brush can be retrofitted to the radiant fin thermal interface (RFTI), baselined as the interface for the International Space Station (ISS) Orbital Replaceable Units (ORU's), without changing the fin structure. Radiant heat transfer is thereby augmented by conductive heat transfer, dramatically increasing total thermal conductance of the interface. ESLI is now addressing critical issues concerning its actual use on the ISS in a Phase 3 program. These issues include carbon fiber debris, mechanical and thermal integrity, mechanical insertion and removal forces, and optimization for best thermal performance. Results thus far are encouraging. In this paper, thermal conductance and insertion/extraction force measurements on prototype specimens are presented.

## INTRODUCTION

Space station batteries and other electronic components must be easily replaceable due to finite lifetimes. These components are packaged as orbital replaceable units (ORU's), replaceable by the crew or through the use of robotics. ORU's generally require thermal contact with the ISS thermal control system in order to maintain component temperatures within required limits. The radiant fin thermal interface (RFTI) has been selected as the ORU thermal interface on the ISS because it is lightweight, separates easily, and avoids the possibility of cold welding in the vacuum of space. The RFTI, developed at Rocketdyne and thermally tested by Peterson and Fletcher (1990), consists of two finned aluminum plates (FAP), which intermesh to exchange heat radiatively. One is mounted on the ISS thermal control system. The mating FAP is mounted on the heat-dissipating ORU. The fins on each plate are 30-mil (0.76 mm) thick, stand 2" (50.8 mm) high, and are spaced 0.250" (6.35 mm) apart. A high-emissivity coating enhances radiation exchange. The vacuum thermal conductance between the intermeshed FAP's at normal operating temperatures is low,  $h \sim 70 \text{ W/m}^2\text{K}$ , (Peterson and Fletcher, 1990), leading to a large temperature difference ( $DT \sim 20 \text{ K}$ ) across the interface during normal operation. This gradient can be substantially reduced by modest conduction between the fins. A lower  $DT$  would result in lower operating temperatures and longer component lifetimes. Alternatively, smaller area radiators, with corresponding weight savings, could be used.

ESLI has engaged in an SBIR program with NASA JSC to develop novel thermal interface materials that are lightweight, compliant, and demonstrate high thermal conductance even for non-flat surfaces. Presently, materials are being evaluated and qualified for use on the ISS under a Phase 3 contract. A rugged, highly compliant brush interface with medium thermal conductance is being tailored for the ISS ORU interface, where the highest conduction materials are not necessary. ESLI's approach is to enhance the RFTI thermal conductance by filling the void between mating fins with a compliant carbon brush to facilitate heat transfer by conduction. Measurements of thermal conductance  $h$  on prototype carbon brush enhanced RFTI's yield vacuum  $h$  values that approach the maximum possible ( $\sim 660 \text{ W/m}^2\text{K}$ ) with current RFTI architecture. By changing the RFTI geometry, e.g. using shorter, thicker Al fins, substantially higher  $h$  values could be attained while at the same time reducing fabrication costs.

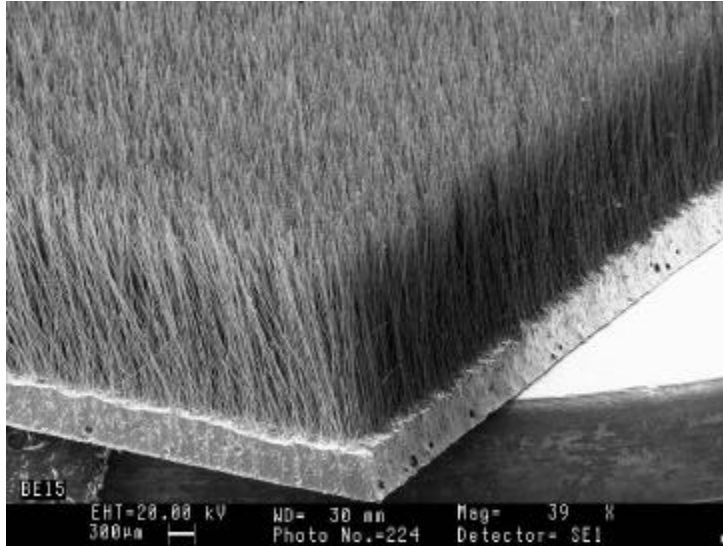


**FIGURE 1.** ESLI carbon fiber brush with vinyl backing.

### **BRUSH FIN THERMAL INTERFACE (BFTI)**

The carbon brush thermal interface consists of numerous PAN carbon fibers (7- $\mu\text{m}$  diameter) oriented perpendicular to the substrate, attached by an adhesive, as shown in Fig. 1. The brush is retrofitted to one of the finned aluminum plates by attaching it to the inside surfaces of the fins with adhesive. The brush interface is lightweight, adding only  $\sim 3 \text{ kg/m}^2$  to the finned aluminum plates, which is 6 % of the mass of the RFTI (Stobb and Limardo, 1992). This brush-enhanced FAP is then intermeshed with the mating FAP by sliding them together, forming what we refer to as a brush fin thermal interface (BFTI). A certain amount of force is required to intermesh because of sliding friction between the fibers and the FAP surface. The fibers must be long enough to span the 2.4-mm distance between intermeshed FAP's, thereby allowing conduction of heat through the carbon fibers. The springy fibers keep the fins of the mating FAP in the center of the gap. A photo of a sample interface, partially intermeshed, is shown in Fig. 2.

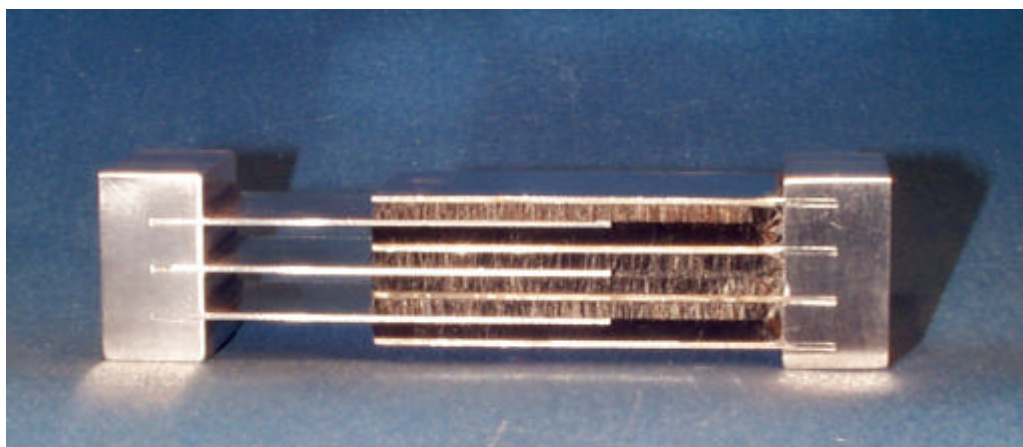


**FIGURE 2.** Small sample brush fin thermal interface (BFTI), consisting of a partially intermeshed FAP pair, one of which has brush attached. The Al fins on each FAP are spaced 0.250" (6.35 mm) apart; each fin has dimensions 0.030" (0.76 mm) thickness x 1" (25.4 mm) width x 2" (50.8 mm) length extension from the plate.

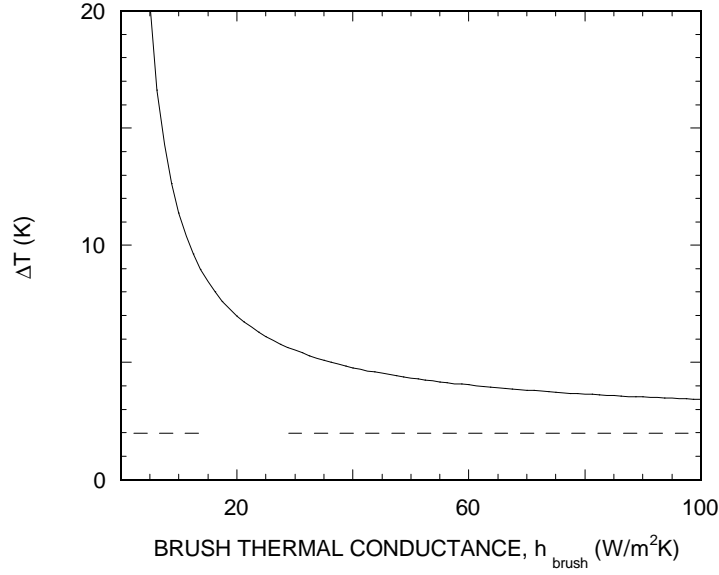


**FIGURE 3.** Temperature difference in degrees Kelvin (Celsius) across the BFTI as a function of brush thermal conductance between adjacent fins,  $h_{brush}$  in  $W/m^2K$ . The solid line represents the theoretical analytical solution of the heat flow model described in the text. The dashed line represents the asymptotic limit of 2 K as  $h_{brush} \rightarrow \infty$ .

## THEORETICAL MODEL

We have found an analytical solution for a model of the BFTI thermal conductance  $h_{BFTI}$  in terms of the thermal conductance  $h_{brush}$  of the carbon brush itself between adjacent fins of the intermeshed BFTI. The model assumes anisotropic thermal conductance of the brush with zero conductance in the direction perpendicular to the fibers, and total conductance  $h_{brush}$  (including contact conductance) in the direction parallel to the fibers. The solution is:

$$h_{BFTI} = n\sqrt{h_{brush}kt} \frac{\sinh \mathbf{f}}{\cosh \mathbf{f} + \mathbf{f} \sinh \mathbf{f}}, \quad \mathbf{f} = L\sqrt{\frac{h_{brush}}{kt}}, \quad (1)$$

where  $n$  is the number of fins per length,  $k$  is the fin thermal conductivity,  $t$  is the fin thickness, and  $L$  is the fin length. Shown in Fig. 3 is a plot of the temperature difference  $DT$  between baseplates of the FAP's, calculated as  $DT = q/h_{BFTI}$  and assuming a heat flux density of  $q = 1400 W/m^2$ . For a perfectly conducting brush ( $h_{brush} \rightarrow \infty$ ),  $DT = 2$  K, which is essentially limited by the 24% fill fraction of the Al fins ( $k = 150 W/mK$ ) in the 50.8-mm gap between the baseplates. For radiant heat transfer between the fins without the carbon brush enhancement,  $DT = 20$  K, using the measured value  $h_{BFTI} = 70 W/m^2K$  (Peterson and Fletcher, 1990). As demonstrated below, a carbon brush with only modest conductance, e.g.  $h_{brush} = 80 W/m^2K$ , results in  $DT = 3.7$  K. Such a brush interface improves conductance by a factor of  $\sim 5$ , approaching the 2 K limit for  $DT$ , and resulting in a significant 16 K lower temperature of the heat-dissipating ORU and attached components.

**TABLE 1.** Properties of PAN carbon fibers used for brush interface samples. Values were taken from manufacturers' specifications.

Fiber Property	Low- $\kappa$ PAN	High- $\kappa$ PAN
Diameter, D ( $\mu m$ )	7.4	6.4
Thermal Conductivity, $\kappa$ (W/mK)	20	267
Tensile Modulus, E (GPa)	227	436

**TABLE 2.** Sample configurations used in testing.

	Sample 1	Sample 2	Sample 3	Sample 4
Fiber type	Low- $\kappa$ PAN	Low- $\kappa$ PAN	Low- $\kappa$ PAN	High- $\kappa$ PAN
Fiber length, L (mm)	2.3	2.5	2.8	2.5
Packing density, $\phi$ (%)	1.0	1.2	1.1	1.4

## EXPERIMENT

### Sample Fabrication

Figure 2 shows the geometry of the BFTI samples made. The fins and plate are made of 6061-T6 Al alloy. The fins are 0.030" (0.76 mm) thick x 1.0" (25.4 mm) wide x 2.25" (57.2 mm) long. They are bonded into 6.4-mm slots machined into the 12.7-mm thick Al base plate with thermally conductive Stycast epoxy such that they extend 2.0" (50.8 mm) from the plate. The mating FAP's consist of 3 and 4 fins, respectively. The carbon brush material was fabricated at ESLI by electroflocking precision-cut (typically within  $\pm 50 \mu\text{m}$ ) carbon fibers into an appropriate adhesive sprayed onto a release liner. After curing, the resulting brush was retrofit to the 4-finned aluminum plate. Two types of commercial PAN carbon fibers were used, one with low thermal conductivity ( $k \sim 20 \text{ W/mK}$ ) and one with higher thermal conductivity ( $k \sim 260 \text{ W/mK}$ ). In general, higher- $\kappa$  carbon fibers have a higher modulus and break more easily than lower- $\kappa$  fibers. Thus, the optimum configuration will be a compromise between the best thermal and mechanical properties. Fiber properties are listed in Table 1. Several sample configurations were made, as summarized in Table 2. The space between evenly spaced, intermeshed fins is 0.095" (2.41 mm). The fibers of Sample 1, which are 2.3-mm long with  $\sim 0.1 - 0.2 \text{ mm}$  adhesive bondline, barely contact the opposing fins. However, this sample was expected to require a minimum amount of force to intermesh. Longer fibers were chosen for the other samples in order to investigate how the thermal conductance and insertion force vary with fiber length.

### Thermal Conductance

The thermal conductance of the fully intermeshed samples was measured using a standard cut-bar steady-state conduction technique. Results were obtained in 1 atm air and in high vacuum ( $\sim 3 \times 10^{-6} \text{ torr} = 4 \times 10^{-4} \text{ Pa}$ ). Two 25.4" x 25.4" square 6061 Al cut bars were used as heat flux meters, one above and one below the sample. The assembly was placed on a water-cooled cold plate that maintained the bottom of the assembly near room temperature. An etched-foil heater mounted at the top of the assembly produced a heat flux of  $15.5 \text{ kW/m}^2$ . Platinum resistance thermometers (RTD's) (1 mm diameter x 25 mm long) were inserted into small diameter holes drilled into the flux meters and in each of the FAP base plates. Thermal grease was used on the RTD's to ensure good thermal contact. The thermal conductance of the BFTI was determined as  $h_{BFTI} = q/DT$ , where  $q$  is the heat flux (in  $\text{W/m}^2$ ) measured by the flux meters and  $DT$  is the temperature difference between the FAP base plates. A correction factor of 8/6 was used to account for the fact that the sample BFTI's have only 6 interfaces instead of 8 per inch for the actual ORU thermal interface. Measured values of  $h_{BFTI}$  in air and in vacuum for Samples 1 - 4 are presented in Table 3. Also shown is  $DT_{BFTI}$ , calculated assuming an operating heat flux density of  $1400 \text{ W/m}^2$  ( $DT_{BFTI} = q/h_{BFTI}$ ), and  $h_{brush}$ , derived from the analytical solution described above. Results for radiant heat exchange from measurements by Peterson and Fletcher (1990) are also shown for comparison. It is clear that all 4 sample configurations provide a significant improvement over that of radiation alone.

The value of  $h_{brush}$  is the result of 3 thermal resistance contributions:  $1/h_{brush} = 1/h_{fibers} + 1/h_{adh} + 1/h_{tips}$ , where  $h_{fibers} = k\ell/L$  is the bulk conductance of the fiber brush (values given in Tables 1 and 2),  $h_{adh}$  is the conductance of the adhesive interface which bonds the fibers to the fins, and  $h_{tips}$  is the interface conductance between the free fiber tips and the opposing fins. It is this last contribution which depends sensitively on the atmospheric conditions (air or

**TABLE 3.** Thermal conductance results. Uncertainty is approx.  $\pm 10\%$ .

	Sample 1	Sample 2	Sample 3	Sample 4	Radiant
$h_{BFTI}$ ( $\text{W/m}^2\text{K}$ ) in air/vac	390/170	400/300	350/250	580/540	70
$DT_{BFTI}$ (K) in air/vac	3.6/8.2	3.5/4.7	4.0/5.6	2.4/2.6	20
$h_{brush}$ ( $\text{W/m}^2\text{K}$ ) in air/vac	85/16	93/43	62/30	900/460	5

**TABLE 4.** Estimates of contributions to  $h_{brush}$ .

	Sample 1	Sample 2	Sample 3	Sample 4
$h_{brush}$ (W/m <sup>2</sup> K) in vac	16	43	30	460
$h_{fibers}$ (W/m <sup>2</sup> K)	87	95	80	1470
$h_{adh}$ (W/m <sup>2</sup> K)	2600	2600	2600	2600
$h_{tips}$ (W/m <sup>2</sup> K) in vac	20 ± 5	80 ± 30	50 ± 16	900 ± 200

vacuum). Rough estimates of the 3 contributions for the thermal vacuum measurements (summarized in Table 3) are given in Table 4. Uncertainty values given for  $h_{tips}$  were calculated assuming  $h_{brush}$  and  $h_{fiber}$  uncertainties of 20%.

It is seen that  $h_{tips}$  is the largest barrier to heat conduction through the carbon brush thermal interface. The  $h_{tips}$  contribution for Sample 1 may be particularly low because in this case the mean fiber length ( $2.30 \pm 0.05$  mm) plus adhesive bondline thickness ( $\sim 0.15$  mm) barely exceeds the fin spacing (2.4 mm). Fibers that are shorter than the mean will not touch the opposing fins, leading to an insulating vacuum gap between fiber tip and fin. Virtually all fibers of Samples 2 – 4 should touch the opposing fins. Values of  $h_{tips}$  for Samples 2 and 3 are the same within their uncertainties. Sample 4, which consists of higher- $\kappa$  PAN fibers, shows a much higher value of  $h_{tips}$ , about an order of magnitude. This is expected considering the formula for a circular spot contact resistance  $R_c$  between two materials of thermal conductivities  $k_1$  and  $k_2$ :

$$R_c = F(a/b)/2ak, \quad (2)$$

where  $a$  is the radius of the contact area,  $b$  is the dimension of the materials, which we take to be the fiber radius ( $\sim 4$   $\mu$ m),  $F(a/b)$  is the constriction alleviation factor which approaches 1 for  $a \ll b$ , and  $k$  is the harmonic mean of the thermal conductivities  $k = 2k_1k_2/(k_1+k_2)$  (Madhusudana, 1996). The harmonic mean for the high- $\kappa$  fibers against Al is 6 times higher than for low- $\kappa$  fibers against Al. In addition, the higher- $\kappa$  fibers are stiffer by a factor of 2, causing them to exert about twice as much pressure against the opposing Al fins as the softer lower- $\kappa$  fibers. This higher pressure results in a higher average area of contact for each fiber (Madhusudana, 1996), and therefore a higher thermal contact conductance by about another factor of  $\sqrt{2}$ .

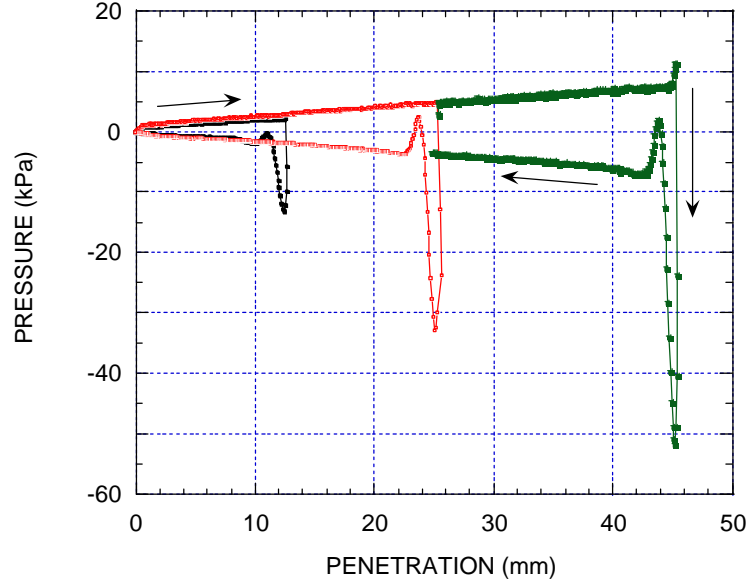


**FIGURE 4.** Pressure required to insert and separate Sample 2 as a function of depth of penetration into mating finned interface. Data are shown for insertion to 13, 25, and 45 mm.

**TABLE 5.** Maximum pressure required to fully intermesh finned aluminum plates (50-mm penetration) against sliding frictional force, and to remove by backing straight out against fiber buckling resistance force.

	Sample 1	Sample 2	Sample 3	Sample 4
Max. Insertion pressure (kPa)	5	8	10	8
Max. Removal pressure (kPa)	30	60	45	50

## Mechanical Properties

The amount of pressure (force per BFTI area) needed to intermesh and separate the FAP sample pairs was measured using an Instron materials testing machine. Shown in Figure 4 is pressure as a function of the interpenetration distance as one FAP was inserted into the other and then removed, at a rate of  $\sim 0.08$  mm/s. Shown are data for Sample 2 for three different penetration depths: 13, 25, and 45 mm. The pressure initially increases rapidly from 0 to 1.4 kPa within the first 0.5 mm as the fibers resist bending until the opposing fins penetrate and start sliding. After that, the pressure increases linearly with penetration depth with slope  $\sim 140$  Pa/mm. In this case, the maximum pressure required to fully insert the two fins 50 mm is  $\sim 8.3$  kPa. As the fins are backed out, the pressure changes sign (since they are being pulled in the opposite direction) and rapidly increases in magnitude, reaching a peak value before decreasing and returning to the value expected for sliding. The resulting large, sharp peak is due to the pressure required to buckle the fibers in order to change the fiber bias direction. Notice that the pressure actually goes positive as the buckled fibers help push the FAP's apart before reaching their preferred bent shape when sliding past the fins being withdrawn.

Fiber buckling can be easily avoided by shifting one of the FAP's in the perpendicular direction before pulling them apart. The shift need be only a fraction of the fiber length ( $\sim 2.5$  mm). In this way, the fibers always slide in the direction of motion. If this is not possible, then the maximum force required is that needed to overcome buckling in order to withdraw the pair. The peak buckling pressure in Fig. 4 is seen to increase approximately linearly with penetration depth with slope  $\sim 1200$  Pa/mm, which is  $\sim 8$  times larger than for sliding. A fully inserted 50-mm long fin configuration would require  $\sim 60$  kPa to remove them. Both the sliding and buckling forces are approximately proportional to the area of brush coverage and can therefore be reduced by applying the carbon brush on only a fraction of the fin area. Similar data were obtained for Samples 1, 3, and 4, with similar features. The main results are given in Table 5.

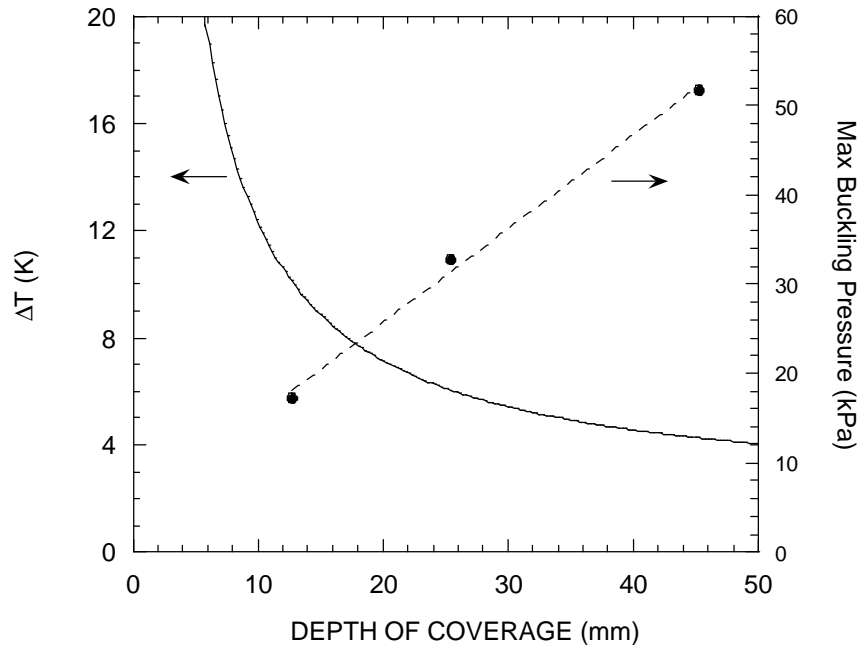


**FIGURE 5.** Temperature drop and maximum buckling pressure as a function of fin coverage for Sample 2. Temperature drop is for a heat flux of  $1.4$  kW/m<sup>2</sup>.

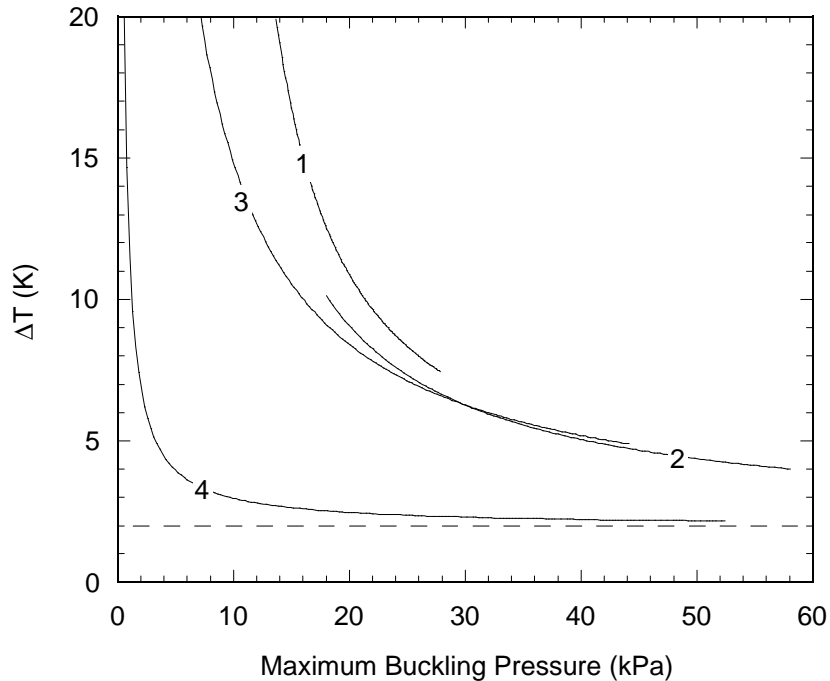


**FIGURE 6.** Temperature gradient across the thermal interface for Samples 1 - 4, plotted as a function of maximum buckling pressure required to remove it. The implicit variable for each curve is the percent coverage of the fins with brush material. The right endpoint of each curve represents performance with full 50.8-mm coverage. The horizontal dashed line represents the lower limit ( $\Delta T = 2$  K) achieved by a perfectly conducting brush ( $h_{brush} \rightarrow \infty$ ).

## SUMMARY

Figure 5 shows both  $\Delta T$  and maximum buckling pressure as a function of coverage for Sample 2. We see that there is a trade-off between obtaining low  $\Delta T$  and low buckling force. The optimum configuration can be chosen with the aid of Fig. 6 which shows  $\Delta T$  vs maximum buckling pressure, with coverage as an implicit parameter. The design engineer should first determine the maximum pressure that can be applied to install/remove the ORU. The approximate  $\Delta T$  can be read from Fig. 6, and will correspond to one (or more) of the brush configurations.

## ACKNOWLEDGMENTS

We are grateful to John Oldson, Phong Liu, and Thomas Bier of ESLI for their technical assistance, and to John Cornwell of NASA JSC for helpful discussions. Work funded by NASA JSC under contracts NAS9-18844, NAS9-19060, and NAS9-97110.

## REFERENCES

- Madhusudana, *Thermal Contact Conductance*, Springer, New York, 1996.
- Peterson, G. P. and Fletcher, L. S., "Determination of the Thermal Contact Conductance and Adhesion Characteristics of Coldplate Thermal Test Pads," P.O. R97PLA-89271802, Test Report to Rocketdyne Div. of Rockwell Int. Corp., April 6, 1990.
- Stobb, C. A. and Limardo, J. G., "Overall Contact Conductance of a Prototype Parallel Fin Thermal Interface", AIAA-92-2846, 1992.